Establishment of the Chemical Equilibria of Different Types of Pyranoanthocyanins in Aqueous Solutions: Evidence for the Formation of Aggregation in Pyranomalvidin-3-O-coumaroylglu...

ARTICLE *in* THE JOURNAL OF PHYSICAL CHEMISTRY B · SEPTEMBER 2010

Impact Factor: 3.3 · DOI: 10.1021/jp1045673 · Source: PubMed

6 AUTHORS, INCLUDING:

Luis Cruz
University of Porto
20 PUBLICATIONS **167** CITATIONS
SEE PROFILE

Natércia Teixeira
University of Porto
19 PUBLICATIONS **181** CITATIONS
SEE PROFILE

F. Pina
New University of Lisbon
205 PUBLICATIONS **3,789** CITATIONS
SEE PROFILE

Establishment of the Chemical Equilibria of Different Types of Pyranoanthocyanins in Aqueous Solutions: Evidence for the Formation of Aggregation in Pyranomalvidin-3-*O*-coumaroylglucoside-(+)-catechin

Luís Cruz,[†] Vesselin Petrov,[‡] Natércia Teixeira,[†] Nuno Mateus,[†] Fernando Pina,[‡] and Victor de Freitas*,[†]

Centro de Investigação em Química, Departamento de Química, Faculdade de Ciências, Universidade do Porto, Rua do Campo Alegre, 687, 4169-007 Porto, Portugal and REQUIMTE, Departamento de Química, Faculdade de Ciências e Tecnologia, Universidade Nova de Lisboa, 2829-516 Caparica, Portugal

Received: May 19, 2010; Revised Manuscript Received: September 9, 2010

The chemical equilibria of the pyranomalvidin-3-glucosides linked to (+)-catechin, (−)-epicatechin, and catechol moieties (and the respective coumaroylglucoside compounds) were established by means of UV−vis spectroscopy. The conjugated double bonds among pyranic rings C and D provide a higher electronic delocalization that prevents the nucleophilic attack of water at position 2. Consequently, besides flavylium cation (AH^+), the bases A, A^-, and A^{2-} have been identified by increasing pH, and the respective acidity constants were determined by spectrophotometry. The formation of dimers at higher concentration was observed for pyranomalvidin-3-*O*-coumaroylglucoside-(+)-catechin, and the respective data treated by the exciton model suggests the formation of a dimer where the monomers form J-type aggregates with the dipolar moments in opposite directions and rotated by 174° at a distance of 5.2 Å (from the center).

Introduction

Pyranoanthocyanins belong to an important group of anthocyanin-derived pigments that occur essentially in processed foodstuffs like fruits and vegetable juices and mainly in red wines.[1] Several different classes of these pigments have been identified in the past decade such as vitisins,[2−4] hydroxyphenylpyranoanthocyanins,[5,6] methylpyranoanthocyanins,[7,8] vinylflavanol-pyranoanthocyanins,[9−11] portisins,[12−14] and more recently a new family of pyranoanthocyanin dimers.[15] Formation of this kind of compounds in food matrixes results from a cycloadition between C-4/5-OH of the anthocyanin and a double bond from another molecule such as pyruvic acid,[4] vinylcatechin,[16] and vinylcatechol,[17,18] resulting in an additional pyran ring D (see Figure 1). Pyranoanthocyanins differ from their genuine precursors (anthocyanins) in many aspects, especially in color. In general, they have a λ_{max} hypsochromically shifted (between 478 and 510 nm) conferring orange colors, except for portisins, which show a bathochromic shift in their λ_{max} values to more bluish hues around 580 nm. Due to their new pyranic ring, the color of these compounds is much more stable toward pH variations and bleaching by SO_2 in comparison to the genuine anthocyanins.[19] In fact, while anthocyanins lose about 80% of their color between pH 1 and 5, as a result of the formation of colorless hemiketal forms (pK_h 2−3), pyranoanthocyanins practically do not change the color intensity.[20] Therefore, they also have the possibility of acting as pseudonatural food colorants in the substitution of synthetic ones. Elucidation of structural transformations that anthocyanin derivatives undergo in aqueous solutions is important in order to understand the color expression of red wines. Formation of pyranoanthocyanins has been appointed by many authors as the main process for which wine color changes from purple to orange-brown during storage and aging.[1] However, their equilibrium forms present in red wine are poorly reported in the literature. For all these reasons and because of the large number of compounds detected in wines so far, pyranoanthocyanin-type compounds have gained great interest. It is well known that the color of anthocyanins is greatly affected by the pH of the solution. The sequence of chemical reactions was correctly established by Brouillard et al.[21−23] using temperature, pressure, and pH jump experiments: at very acidic pH, the red flavylium cation (AH^+) is the predominant species; when the pH is raised the flavylium cation immediately undergoes a proton transfer reaction, giving rise the purple quinonoidal base (A), and simultaneously but more slowly the flavylium cation leads formation of colorless hemiketal (B) in the hydration reaction. The hemiketal compound further undergoes a tautomerization reaction to give the pale yellow *cis*-chalcone (Cc), which isomerizes to *trans*-chalcone (Ct). However, these authors gave less importance to formation of Ct (minor species in common anthocyanins at room temperature). After the works of McClelland (1980)[24] and Preston and Timberlake (1981)[25] in which *trans*-chalcone was identified and isolated, complete elucidation of all pH-dependent species of malvidin-3,5-diglucoside was carried out by Santos et al. (1993).[26] Recently, Asenstorfer et al. (2003)[27] determined by electrophoresis studies that the first proton transfer reaction of malvidin 3-glucoside occurs at a quite lower pH (pK_a 1.76) than the ones previously reported (3.7 and 4.3),[22,28] which is controversial. Besides, similar results published with vitisin A and B are also somehow divergent. For example, Asenstorfer et al. (2007)[29] determined two pK_h values for vitisin A by absorption spectroscopy, while Oliveira et al. (2009)[30] by means of NMR and visible spectroscopy reported that the hydration reaction does not occur in vitisin B. In this work, six different types of pyranoanthocyanins were studied by UV−vis spectroscopy in order to comprehend what kind of chemical

* To whom correspondence should be addressed. Phone: +351.226082862. Fax: +351.226082959. E-mail: vfreitas@fc.up.pt.
[†] Centro de Investigação em Química.
[‡] REQUIMTE.

10.1021/jp1045673
Published on Web 09/29/2010

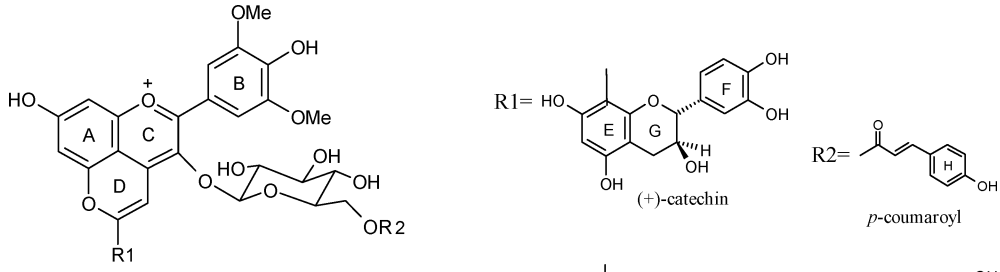

1: R1=(+)-catechin, R2=H
2: R1=(+)-catechin, R2=*p*-coumaroyl
3: R1=(-)-epicatechin, R2=H
4: R1=(-)-epicatechin, R2=*p*-coumaroyl
5: R1=catechol, R2=H
6: R1=catechol, R2=*p*-coumaroyl

Figure 1. Structures of the pyranoanthocyanin pigments (**1**−**6**) studied.

equilibrium could be established and provide the respective equilibrium thermodynamic constants. This knowledge will allow predicting which species of this type of pyranoanthocyanins could occur at wine pH and how they may contribute to the red wine color. (Usually in a monomer−dimer equilibrium the mathematical definition of the mole fraction of the dimer is 2[D]/([M] + 2[D]) while the mole part, [D]/([M] + [D]), and *mutatis mutandis* for the monomer. In common equilibria these definitions are coincident and used without distinction.)

Materials and Methods

Reagents. TSK Toyopearl gel HW-40(S) was purchased from Tosoh (Tokyo, Japan). Malvidin-3-*O*-glucoside (mv3glc) and malvidin-3-*O*-coumaroylglucoside (mv3coumglc) were isolated from a young red table wine (*Vitis vinifera* L. cv. Touriga Nacional) by semipreparative HPLC using a reversed-phase C18 column (250 mm × 4.6 mm i.d.) as reported elsewhere.[31] 8-Vinyl-(+)-catechin, 8-vinyl-(−)-epicatechin, and 4-vinylcatechol were obtained through organic hemisynthesis from (+)-catechin, (−)-epicatechin, and catechol, respectively, following a strategy already reported.[32] The structures of these compounds were assessed by NMR by comparison with the data previously published.[17,32] Acetonitrile (HPLC grade) and ethanol (absolute) were obtained from Carlo Erba (Val de Reuil, France); formic acid (98%, PA-ACS) and methanol (99.5%) were purchased from Panreac Química Sau (Barcelona, Spain); hydrochloridric acid (37% v/v), sodium hydroxide, and ethyl acetate were purchase from José M. Vaz Pereira, S.A. (Lisboa, Portugal). A universal buffer of Theorell and Stenhagen[33] was made by dissolving 2.25 mL of phosphoric acid (85% w/w), 7.00 g of monohydrated citric acid, 3.54 g of boric acid, and 343 mL of 1 M NaOH solution in Millipore water to 1 L. Solutions were made using Millipore water. All other chemicals used were HPLC grade.

Hemisynthesis of Pyranoanthocyanin Pigments. The hemisyntheses of six pyranoanthocyanin-type pigments were proceeded through the procedures described elsewhere.[16,17] Briefly, solutions containing mv3glc or mv3coumglc (2.5 mM) were incubated with 8-vinyl-(+)-catechin, 8-vinyl-(−)-epicatechin, or 4-vinylcatechol (2−3 equiv) in 5−10% ethanol/water at pH 3.5 (adjusted with dilute HCl or NaOH) at 30 °C. Formation of the respective pigments was monitored by high-performance liquid chromatography (HPLC) with diode array detection (DAD) at 500 nm. When their formation reached the maximum, the reactions were stopped and the respective purifications were performed.

Pigment Purification. The ethanol of each solution was eliminated by evaporation, and liquid−liquid extraction with ethyl acetate was performed in order to remove the catechins and other organic impurities. The aqueous phases containing the pyranoanthocyanin derivatives were applied onto a TSK Toyopearl gel HW-40 (S) column (250 mm × 16 mm i.d.), and the pigments were eluted with 40−50% aqueous methanol acidified with 2% HCl at a flow rate of 0.8 mL/min. The fractions collections were made upon visual detection of the colored bands. Methanol was removed under vacuum, protected from light and at room temperature. The pyranoanthocyanin pigments were freeze dried and then stored at −18 °C until use. When necessary, preparative HPLC was used in order to obtain pure pigments. The compounds were further characterized by LC-DAD/ESI-MS, and their structures and purity were assessed by NMR analyses.[11,17,34]

HPLC. The samples were analyzed by HPLC (Merck-Hitachi L-7100) on a 150 mm × 4.6 mm i.d. reversed-phase C18 column (Merck, Darmstadt, Germany) thermostatted at 25 °C; detection was carried out at 500 nm using a diode array detector (Merck-Hitachi L-7450A). Solvents were (A) water/formic acid 9:1 (v:v) and (B) acetonitrile with the following gradient: 10−35% B over 50 min at a flow rate of 0.5 mL/min. The sample injection volume was 20 μL. The chromatographic column was washed with 100% B for 10 min and then stabilized with the initial conditions for another 10 min.

The preparative HPLC system (Elite LaChrom) was composed of a L-2130 quaternary pump, a manual injector with a loop of 250 μL, and a L-2420 UV−vis detector. The stationary phase was composed of a reversed-phase C18 column (Merck, Darmstadt, Germany) (150 mm × 4.6 mm i.d., 5 μm pore size) thermostatted at 25 °C, and the eluents were (A) water/formic acid 9:1 (v:v) and (B) methanol with the following gradient: 20−100% B over 60 min at a flow rate of 1 mL/min. The detection wavelength was set to 500 nm.

LC-DAD/ESI-MS Analysis. A Finnigan Surveyor series liquid chromatograph equipped with a Thermo Finnigan (Hypersil Gold) reversed-phase column (150 mm × 4.6 mm, 5 μm, C18) thermostatted at 25 °C was used. The samples were analyzed using the same solvents, gradients, injection volume, and flow rate referred to above for HPLC analysis. Double-online detection was done by a photodiode spectrophotometer and mass spectrometry. The mass detector was a Finnigan LCQ DECA XP MAX (Finnigan Corp., San Jose, CA) quadrupole ion trap equipped with an atmospheric pressure ionization (API) source, using an electrospray ionization (ESI) interface. The

vaporizer and capillary voltages were 5 kV and 4 V, respectively. The capillary temperature was set at 325 °C. Nitrogen was used as both sheath and auxiliary gas at flow rates of 90 and 25, respectively (in arbitrary units). Spectra were recorded in positive-ion mode between *m/z* 250 and 1500.

NMR Analysis. ^{1}H NMR (500.13 MHz) and ^{13}C NMR (125.77 MHz) spectra were recorded in CD_3OD/TFA (98:2) on a Bruker-Avance 500 spectrometer at 303 K and with TMS as an internal standard (chemical shifts (δ) in parts per million, coupling constants (J) in Hertz). Multiplicities are recorded as singlets (s), doublets (d), triplets (t), doublets of doublets (dd), multiplets (m), and unresolved (*). ^{1}H chemical shifts were assigned using 2D NMR (COSY) experiments, while ^{13}C resonances were assigned using 2D NMR techniques (*g*HMBC and *g*HSQC).[35,36] The delay for the long-range C/H coupling constant was optimized to 7 Hz.

Absorption Spectroscopy. UV−vis absorption spectra were recorded on a Varian-Cary 100 Bio spectrophotometer. Spectroscopic absorbance curves were recorded at 25 °C for all of the solutions from 200 to 800 nm with a 1 nm sampling interval using a quartz cell cuvette of 3.5 mL capacity and 1 cm optical path.

Determination of the Thermodynamic Pseudoequilibrium: Apparent Acidity Constant (K'_a). Stock solutions of pyranoanthocyanin pigments (0.1 mM) were prepared in 10% ethanol/aqueous solution of 0.1 M HCl, which was kept, protected against the sunlight, at 4 °C. The resulting low pH value of the stock solutions (pH ≈ 1) ensured that most of the pyranoanthocyanins is in its flavylium form, thus preventing pigment degradation.

Determination of the apparent acidity constant (thermodynamic pseudoequilibrium) was accomplished by measuring, on the common UV−vis spectrophotometer, solutions composed of one-third of a pyranoanthocyanin stock solution, one-third of a solution of NaOH (0.1 M), and one-third of a universal buffer solution (with 20% ethanol) at pH's of 3, 5, 7, 9, and 11.

Titrations. The acidic thermodynamic constants were determined by spectophotometric titrations. Subsequently added to the cell cuvette were 1 mL of NaOH solution (0.1 M), 1 mL of universal buffer solution (with 20% ethanol) at pH 3, and 1 mL of a stock solution of the pyranoanthocyanins, where the final concentration of each pigment was 0.03 mM. The first UV−vis spectrum was immediately recorded. Increasing amounts of NaOH solutions 10 or 1 M were successively added to the cell cuvette, achieving a pH range between 3 and 12. After each addition, the mixture was rapidly shacked, a UV−vis spectrum was recorded, and the pH was measured. Final volumes were appropriately corrected.

pH Measurements. All pH measurements were made in a Crison micro pH meter 2002 fitted with a Crison 5209 electrode. The calibration was made with standard buffers pH 7.0 and 4.0 purchased from Crison.

Aggregation of Pigment 2. A highly concentrated stock solution of pigment **2** (~1 mg in 500 μL) was prepared in a 10% ethanol/aqueous solution of 0.1 M HCl (pH = 1.3), and a UV−vis spectrum was recorded using a quartz cell cuvette with a 0.2 cm optical path. Increasing volumes of solvent were added to the stock solution, and after each dilution a UV−vis spectrum was recorded. When the absorbance at λ_{max} reaches 0.45, the following UV−vis spectra were recorded using a quartz cell cuvette with a 1 cm optical path until a 40 times dilution had been reached.

Results and Discussion

Hemisynthesis of Pyranoanthocyanin Pigments. Six different types of pyranoanthocyanin pigments **1**−**6** were synthesized in model solution through the reactions of the respective anthocyanin (malvidin-3-*O*-glucoside or malvidin-3-*O*-coumaroylglucoside) with 8-vinyl-(+)-catechin, 8-vinyl-(−)-epicatechin, and 4-vinylcatechol (Figure 1), according to previous studies.[16,17,32]

TABLE 1: Mass and Spectroscopic Data of the Synthesized Pyranoanthocyanins

pigments	λ_{max} (nm)[a]	$[M]^+$, *m/z*	MS^2, *m/z*	MS^3, *m/z*
pymv3glc-(+)-catechin, **1**	505	805	643	491
pymv3coumglc-(+)-catechin, **2**	502	951	643	491
pymv3glc-(−)-epicatechin, **3**	505	805	643	491
pymv3coumglc-(−)-epicatechin, **4**	508	951	643	491
pymv3glc-catechol, **5**	502	625	463	447
pymv3coumglc-catechol, **6**	505	771	463	447

[a] Recorded from the LC-DAD.

After the purification steps, the pure pigments were individually analyzed by LC-DAD/ESI-MS in positive-ion mode (Table 1). Full ^{1}H and ^{13}C NMR characterization confirmed the structures of pigments **1**−**6**, which are in agreement with the data already described in the literature.[11,17,34]

UV−vis spectra of the synthesized pigments recorded from the LC-DAD revealed an absorbance maximum λ_{max} between 502 and 508 nm, which is typical of pyranoanthocyanin compounds.[37] Additionally, spectra of pigments **2**, **4**, and **6** show a shoulder around 310 nm, which is characteristic of acylation of *p*-coumaric acid.[38]

Thermodynamic Equilibrium. In the case of natural anthocyanin compounds, it is well known that the flavylium cation, AH^+, is thermodynamically stable at very acidic pH values (pH = 1), being the dominant species of the equilibrium (Figure 2). When the pH becomes higher, the flavylium cation could be involved in two parallel reactions: (i) acid−base reaction to form the neutral quinonoidal base, A, and (ii) hydration reaction to give the colorless hemiketal, B. Proton transfer reactions take place immediately after the pH jump on a microseconds time scale, while the hydration reaction is much slower (subseconds to seconds). On the other hand, at higher pH values (moderately acidic) A is not the most stable species at the equilibrium but B, which means that A is formed during the first instants of the process and disappears partially later to give the equilibrium distribution at these pH values, including also minor fractions of Cc and Ct (Figure 2).

In order to study what kind of reactions pyranoanthocyanins undergo, pH jumps from 1 to 3, 5, 7, 9, and 11 were carried out. The respective UV−vis absorption spectra were recorded and the kinetic processes followed over time. The shape and position of the absorption bands do not change significantly after 70 h, which is indicative of the stability of the structures and means that no chemical transformations/degradations may occur during this period (see Figure 9 in the Supporting Information).

However, during this large period of time a continuous decrease of the absorbance was observed in a wide range of wavelengths for each pH. This behavior was initially thought to be due to a very slow hydration process that could occur preferentially in the positively charged carbon 2 since the other active positions (carbons 4 and 10) are blocked. Later, it was concluded that the observed behavior is due essentially to precipitation of the compounds. In fact, after some days, some solid particles were observed at the bottom of the flasks. However, despite a greater decrease in the absorbance intensity observed at pH 3 (see Figure 9 in the Supporting Information), there were more solid particles mainly at pH 5 and 7, where

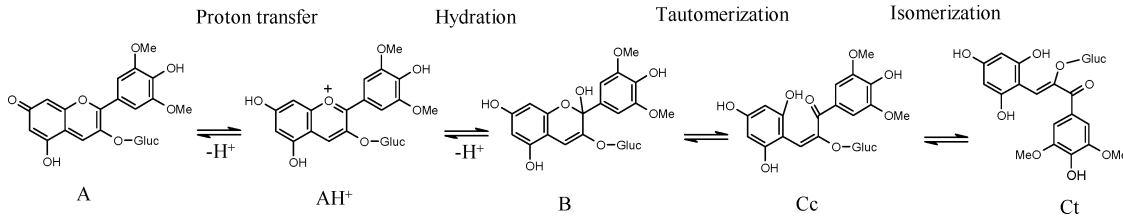

Figure 2. Equilibrium forms of natural anthocyanins in aqueous solutions.

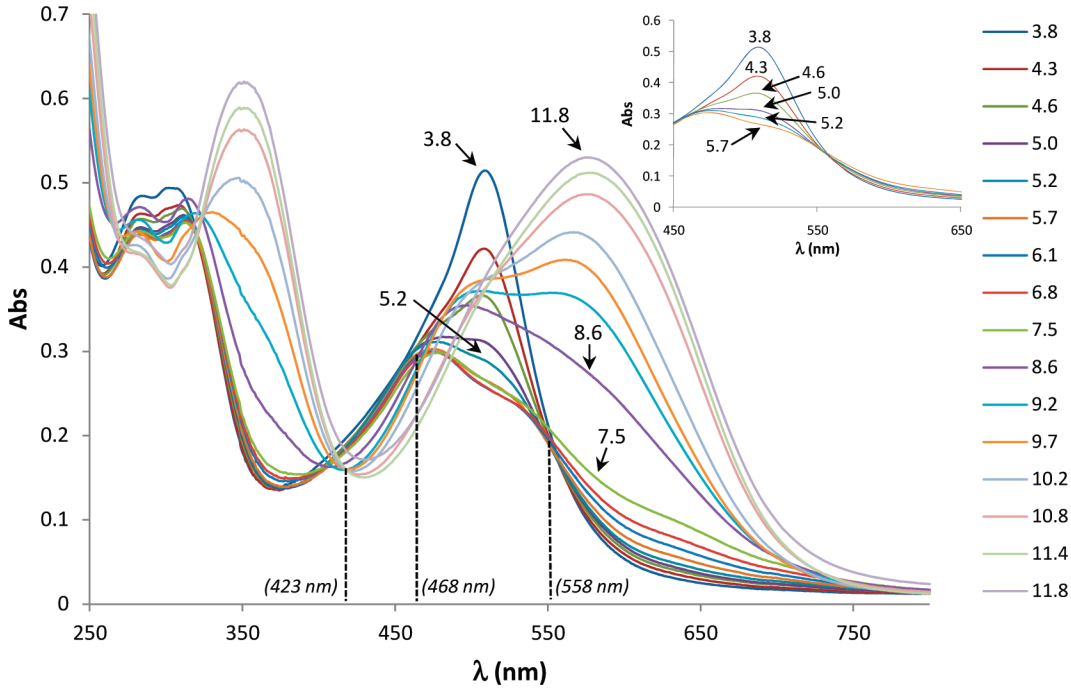

Figure 3. UV−vis spectra of the solutions of pyranomv3coumglc-catechol pigment **6** at different pH values between 3.8 and 11.8. (Inset) UV−vis spectra of the same pigment from 450 to 650 nm at pH values between 3.8 and 5.7.

the concentration of neutral quinonoidal base A is higher. The conjugated double bonds among the pyranic rings C and D seem to provide a higher electronic delocalization that should avoid nucleophilic attack of water at position 2.

Figure 3 show the evolution of the UV−vis spectra of solutions of pyranomv3coumglc-catechol pigment **6** at different pH measured immediately after pH change. As pH increases an isosbestic point was found around 558 nm, which is indicative of the neutral quinonoidal base appearance (see inset of Figure 3).

Once again, no evidence of the hydration process was observed immediately after the pH increase from slightly acid to neutral. Indeed, some reverse pH jump experiments were performed in the stopped flow equipment in order to determine amounts of hemiketal. A solution of the compound (initially at pH = 1.0) was left at pH = 6.0 for approximately 30 min, and a pH jump back to acid was followed by stopped flow (reverse pH jumps). Observation of a small increase of the flavylium absorption within the lifetime of seconds does not exclude formation of residual amounts of hemiketal. This process was neglected due to its small amplitude.

Furthermore, no evidence of formation of B_2 hemiketal (appearance of a band with an absorption at 280 nm, see Figure 9 in the Supporting Information) is given in the recorded UV−vis spectra. A similar behavior was observed for all compounds studied. This means that only acid−base reactions should take place as recently reported for vitisin B-type compounds by UV−vis and NMR studies.[30]

Determination of pK_a Values. Titrations of all pigments were performed in order to determine the respective pK_a values. The titration was fast enough to avoid significant precipitation, which is a relatively slow process. The UV−vis spectrum of each pigment was obtained for the range of pH between 3 and 12 (for example, for pigment **6**, Figure 3).

Overall, by increasing the pH the following behavior was observed for all pigments: a decrease in the absorbance accompanied by a blue shift of λ_{max} followed by an absorbance increase with a red shift of λ_{max}.

For pigment **6**, the first isosbestic point was achieved at approximately 558 nm and can be attributed to the equilibrium between AH^+ and A. The second isosbestic point was found around 468 nm and is due to the equilibrium between A and A^- species, while the third isosbestic point (423 nm) is related to the equilibrium between A^- and A^{2-}.

Treatment of the experimental data reported in Figure 3 using a simple mathematical decomposition allowed achieving the UV−vis absorption spectra of the four species, AH^+, A, A^-, and A^{2-} (see the cases of pigments **1** and **2**, Figure 4).

For pigment **1**, the first species formed is the neutral quinonoidal base (A) which displays a λ_{max} hypsochromatically shifted (~477 nm) in comparison with AH^+. The second deprotonation lead to the anionic quinonoidal base (A^-), bathochromatically shifted ($\lambda_{max} \approx 557$ nm). The third species formed is the dianionic quinonoidal base, A^{2-}, which is blue ($\lambda_{max} \approx 574$ nm).

In Figure 4II, it is interesting to note that the A^{2-} species showed a band with λ_{max} around 360 nm. This behavior was

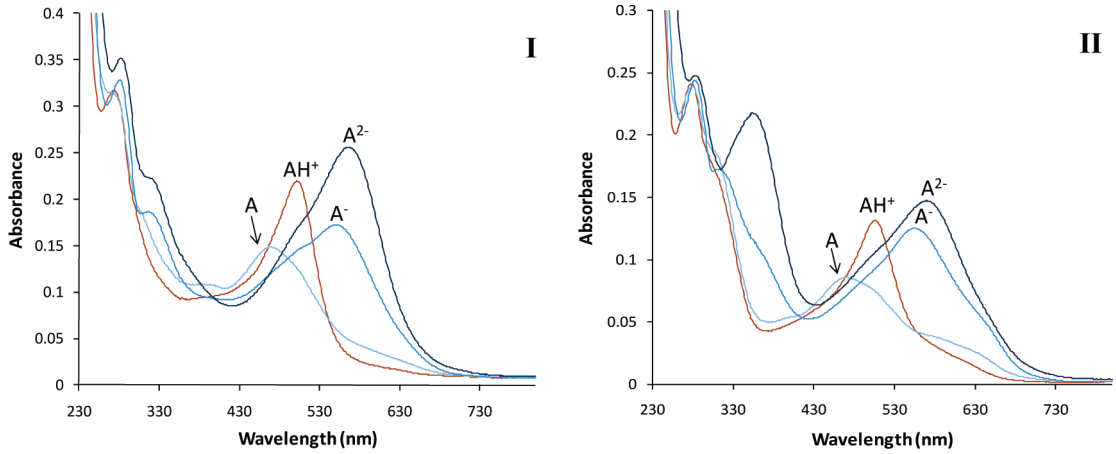

Figure 4. UV−vis spectra of the individual species of the pigments pyranomv3glc-(+)-catechin **1** (I) and pyranomv3coumglc-(+)-catechin **2** (II).

only observed for pigments **2**, **4**, and **6** which have a *p*-coumaroyl residue attached. In fact, when the A^{2-} species is formed (pH > 9.5), the ionized form of the *p*-coumaroyl residue is already present in solution (pK_{a2} *p*-coumaric acid = 8.98),[39] which might contribute to the appearance of a band at 360 nm.

On this basis, the flavylium cation can be considered as a three protic acid and the global process can be accounted for by eqs 1−3

$$AH^+ + H_2O \leftrightarrow A + H_3O^+ \quad K_{a1}\text{, first proton transfer} \tag{1}$$

$$A + H_2O \leftrightarrow A^- + H_3O^+ \quad K_{a2}\text{, second proton transfer} \tag{2}$$

$$A^- + H_2O \leftrightarrow A^{2-} + H_3O^+ \quad K_{a3}\text{, third proton transfer} \tag{3}$$

$$K_{a1} = \frac{[A][H_3O^+]}{[AH^+]}$$
$$K_{a2} = \frac{[A^-][H_3O^+]}{[A]}$$
$$K_{a3} = \frac{[A^{2-}][H_3O^+]}{[A^-]} \tag{4}$$

The total concentration of individual species, C_0, is given by eq 5

$$C_0 = [AH^+] + [A] + [A^-] + [A^{2-}] \tag{5}$$

and the mole fraction distribution of the different species, χ_i, is calculated as follows

$$\chi_{AH^+} = \frac{[AH^+]}{C_0} = \frac{[H_3O^+]^3}{[H_3O^+]^3 + K_{a1}[H_3O^+]^2 + K_{a1}K_{a2}[H_3O^+] + K_{a1}K_{a2}K_{a3}} \tag{6}$$

$$\chi_A = \frac{[A]}{C_0} = \frac{K_{a1}[H_3O^+]^2}{[H_3O^+]^3 + K_{a1}[H_3O^+]^2 + K_{a1}K_{a2}[H_3O^+] + K_{a1}K_{a2}K_{a3}} \tag{7}$$

$$\chi_{A^-} = \frac{[A^-]}{C_0} = \frac{K_{a1}K_{a2}[H_3O^+]}{[H_3O^+]^3 + K_{a1}[H_3O^+]^2 + K_{a1}K_{a2}[H_3O^+] + K_{a1}K_{a2}K_{a3}} \tag{8}$$

$$\chi_{A^{2-}} = \frac{[A^{2-}]}{C_0} = \frac{K_{a1}K_{a2}K_{a3}}{[H_3O^+]^3 + K_{a1}[H_3O^+]^2 + K_{a1}K_{a2}[H_3O^+] + K_{a1}K_{a2}K_{a3}} \tag{9}$$

The absorbance at wavelength λ shows a pH dependence which is given by the following equation

$$A_{calcd} = \varepsilon_{AH^+}\chi_{AH^+} + \varepsilon_A\chi_A + \varepsilon_{A^-}\chi_{A^-} + \varepsilon_{A^{2-}}\chi_{A^{2-}} \tag{10}$$

where ε_{AH^+}, ε_A, ε_{A^-}, and $\varepsilon_{A^{2-}}$ are the mole absorption coefficients of the individual species or components at the considered wavelength.

The pK_a values were determined by fitting the calculated absorbance values by eq 10 to the ones obtained experimentally. The solver function was then used to minimize the sum of the difference between the theoretical and the experimental values squared.

In Figure 5, the molar fractions of each species and the experimental absorbance values at two chosen wavelengths are plotted for pigment **1**, with the respective fittings, as a function of pH.

The pK_a values for pigments **1**−**6** are given in Table 2. It is reported in the literature that the pK_a for 7-hydroxyflavylium is 3.55 while in 4′-hydroxyflavylium is 4.5. Therefore, it is easier to remove a proton from position 7 than from position 4′. When

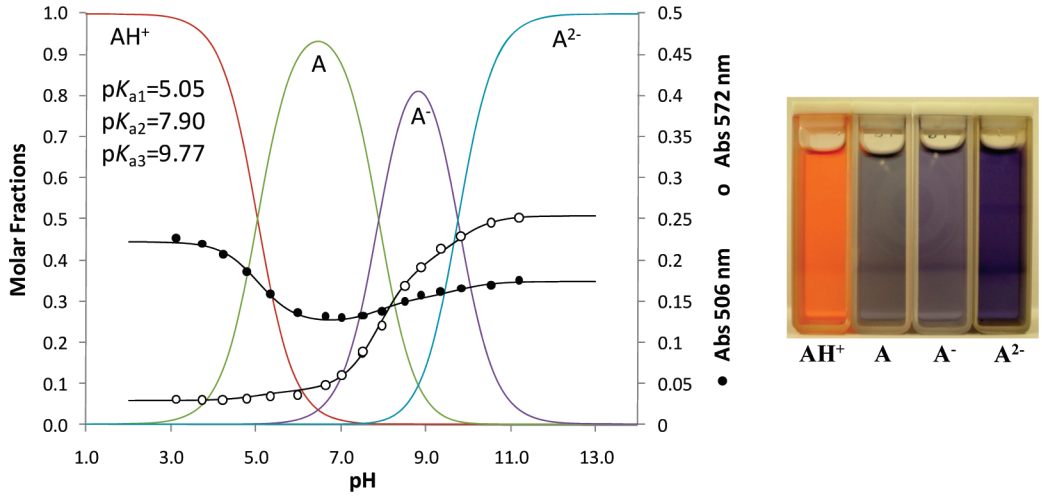

Figure 5. Determination of respective pK_a values of pigment **1** at λ = 506 and 572 nm. The cuvette cells show the colors of each individual species.

TABLE 2: pK_a Values for Pigments 1−6 Obtained from UV−Vis Spectroscopy[a]

	AH^+	A		A^-		A^{2-}	
pigment	λ_{max} (nm)	pK_{a1}	λ_{max} (nm)	pK_{a2}	λ_{max} (nm)	pK_{a3}	λ_{max} (nm)
1	507	5.05 (±0.05)	477	7.90 (±0.07)	557	9.77 (±0.06)	574
2	512	5.35 (±0.08)	480	8.06 (±0.09)	562	9.76 (±0.07)	577
3	508	4.80 (±0.09)	481	7.82 (±0.09)	567	9.49 (±0.10)	576
4	509	5.24 (±0.11)	476	8.02 (±0.10)	559	9.60 (±0.08)	577
5	511	4.20 (±0.06)	487	7.84 (±0.05)	577	10.28 (±0.07)	583
6	513	4.31 (±0.07)	471	8.34 (±0.06)	562	10.20 (±0.06)	583

[a] Values in parentheses are the standard deviations of the curve-fitting procedure.

two hydroxyl groups are present, release of the first proton influences the pK_a of the second one and successively. For example, in the case of 7,4′-dihydroxyflavylium, the first (7-OH) pK_a is 4 while the second (4′-OH) is 8,[40−43] which are in agreement with the ones obtained for all pigments studied (pK_{a1} 4.20−5.35 and pK_{a2} 7.82−8.34). This data also agrees with the pK_a values obtained for the vitisin B pigment which has the same pyranoflavylium core in its structure.[30] The third pK_a obtained for the pigments bearing a (+)-catechin or (−)-epicatechin moiety (**1**−**4**) is observed between 9.49 and 9.77, and the two pK_a values for catechin and epicatechin described in the literature are 8.16 and 9.20.[44] The third pK_a for the pigments with catechol moieties (**5** and **6**) are higher (around 10.20), which is consistent with the catechol pK_a values reported in aqueous solutions (pK_{a1} 9.45 and pK_{a2} 12.8).[45] Overall, the pigments that bear a coumaroyl residue (**2**, **4**, and **6**) revealed slightly higher pK_a values than the respective glucosides (**1**, **3**, and **5**), which may be explained by the higher steric hindrance brought by the coumaroyl group to the overall structure, making it more difficult to remove an additional proton.

The general equilibrium forms of the pyranoanthocyanins studied in aqueous solutions for the pH range between 3 and 12 are depicted in Figure 6.

Aggregation of Pigment 2. Aggregation of the ionic dyes in solution is one of the properties which affects their spectral and physicochemical properties.[46,47] It is well known that these compounds form dimers even at very low concentrations from 10^{-5} to 10^{-6} M.[48]

Formation of aggregates was only observed for pigment **2** by recording the UV−vis spectrum of the stock solution (0.1 mM), which showed two bands with a λ_{max} bathochromatically shifted from 509 to 526 nm. The UV−vis spectrum of this diluted solution (5×10^{-5} M) was then recorded, resulting in the appearance of only one band (λ_{max} 509 nm). This observation is indicative of a monomer−dimer equilibrium.

In order to characterize the monomer−dimer equilibrium, several UV−vis spectra of pigment **2** were recorded as a function of increasing concentrations from 5.7×10^{-5} to 2.6×10^{-4} M (Figure 7A). The absorbance data that would be obtained for the initial concentration C_0 and for an optical path of 1 cm were appropriately corrected (Figure 7B).[49]

Two sets of isosbestic points were clearly identified, suggesting not only formation of a dimer but also high-order aggregates, as can be confirmed from Figure 10 of the Supporting Information.

Calculation of the monomer−dimer equilibrium was achieved taking into account only the points where the absorption can be considered linearly dependent on the logarithm of the concentration, and the high-order aggregates could be neglected.

The monomer (M)−dimer (D) equilibrium is described by eq 11

$$M + M \leftrightarrow D \tag{11}$$

and the dimeric constant (K_D) is defined by eq 12

$$K_D = \frac{[D]_{eq}}{([M]_{eq})^2} = \frac{\chi_{eq}^D}{2C_i^0(\chi_{eq}^M)^2} \tag{12}$$

Considering the mass balance of the system is given by eq 13

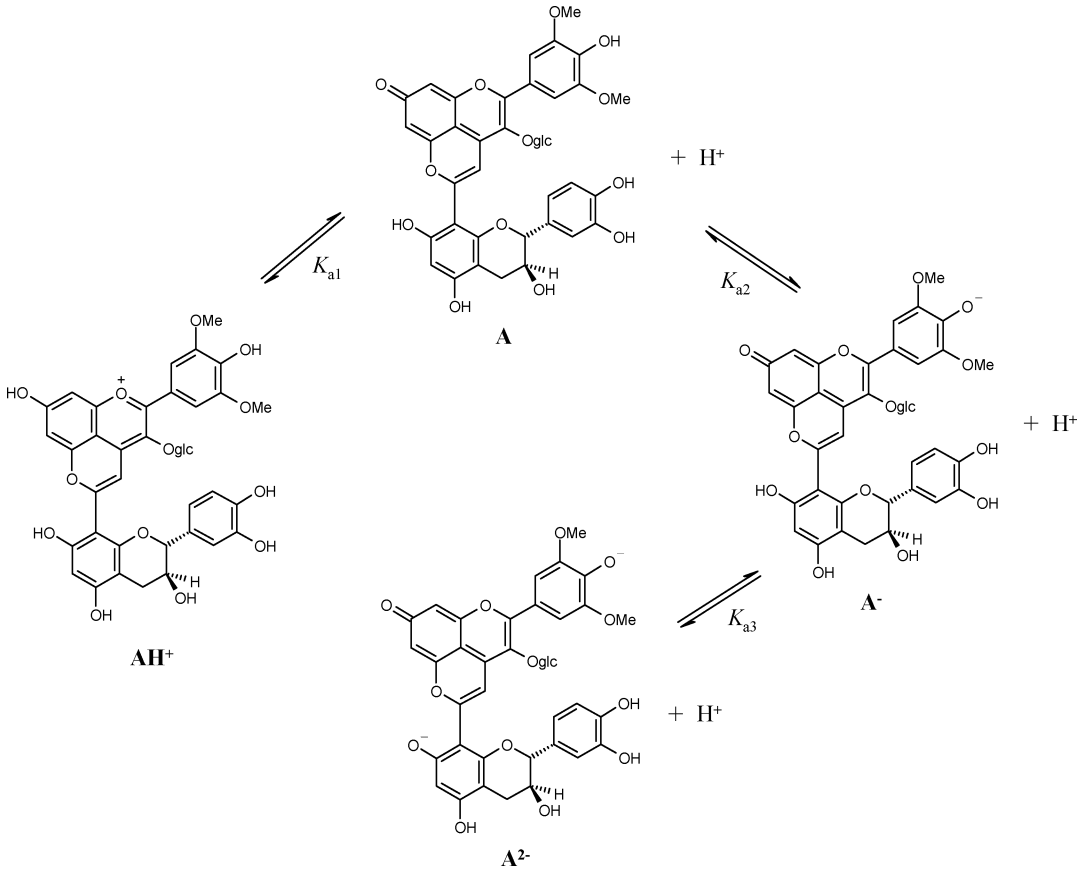

Figure 6. Equilibrium forms of pyranomv3glc-(+)-catechin pigment **1** in aqueous solutions for the pH range between 3 and 12.

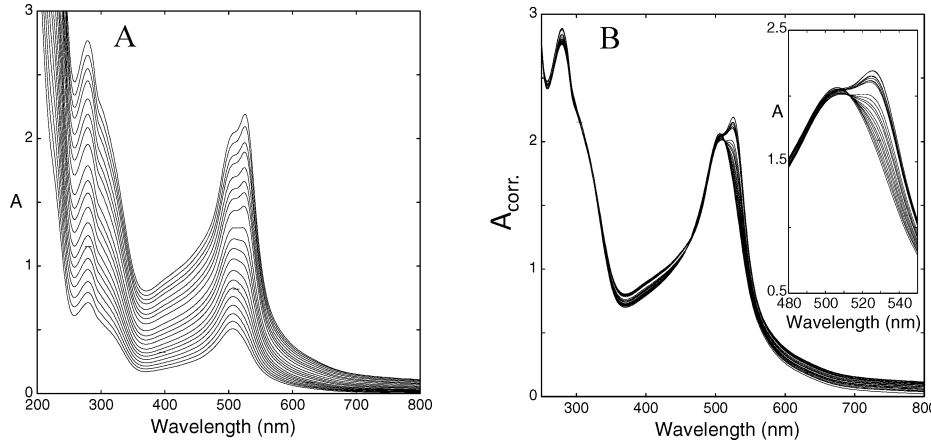

Figure 7. (A) Absorption spectra of pigment **2** as a function of the concentration from 5.7×10^{-5} to 2.6×10^{-4} M; (B) UV−vis spectra of pigment **2** solutions with different concentrations keeping $C_0 l$ constant.

$$\chi_{eq}^{M} + \chi_{eq}^{D} = 1$$

$$[M]_{eq} + 2[D]_{eq} = C_i^0 \qquad (13)$$

where the molar fractions (χ) are defined according eqs 14 and 15

$$\chi_{eq}^{M} = \frac{[M]_{eq}}{C_i^0} = \frac{-1 + \sqrt{1 + 8C_i^0 K_d}}{4K_d C_i^0} \qquad (14)$$

$$\chi_{eq}^{D} = \frac{2[D]_{eq}}{C_i^0} \qquad (15)$$

$$A = A_M \chi_{eq}^{M} + A_D \chi_{eq}^{D} \qquad (16)$$

where A_M and A_D are the absorptions that the pure species would have at an initial concentration C_i^0 and at 526 nm.

The fitting was achieved using eqs 13−16 for $\log K_d = 3.5 \pm 0.1$, and ϵ_M and ϵ_D are equal to 12 600 and 53 000 M^{-1} cm^{-1}, respectively ($A_D = (\varepsilon_D C_i^0)/2$ and $A_M = \varepsilon_M C_i^0$) (Figure 8A and see Figure 11 in the Supporting Information).

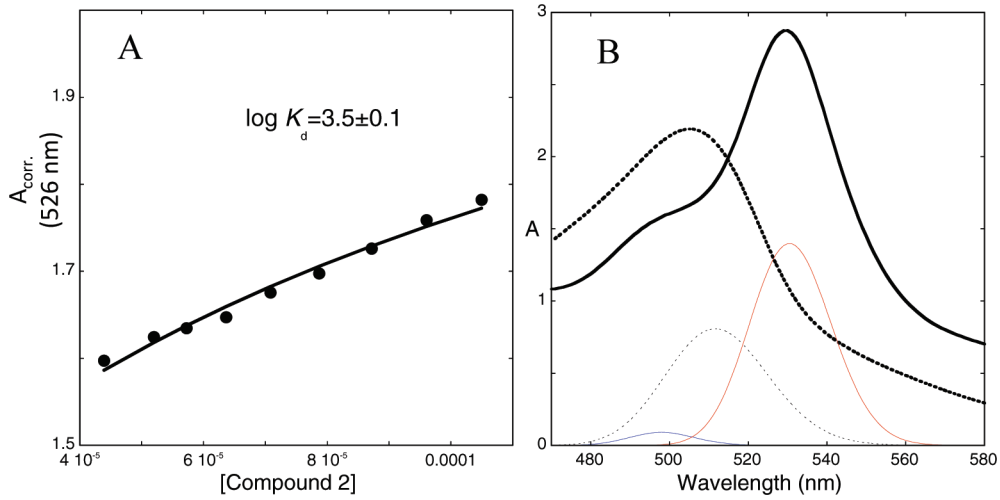

Figure 8. (A) Fitting of the absorption of compound **2** at 526 nm using eqs 14−16. (B) Calculated monomer (dotted line) and dimer (full line) individual absorption spectra of pigment **2**. Decomposition bands used for calculation of the dimer parameters are also represented.

TABLE 3: Results for Parameters of the Dimer Formed by Pigment 2

	pigment **2**
$\Delta\nu$ (cm^{-1})	1232
α (deg)	174
R (Å)	5.2
log K_D	3.5

The set of absorption spectra regarding the monomer−dimer equilibrium were proceeded by the FiNAl algorithm[50] as described in ref 49. This algorithm recovers the individual spectrum of the monomer and dimer and gives their contribution (mole fraction) for each concentration. Moreover, the overall spectrum of the monomer and dimer is resolved in their individual bands (Gaussian shape) (Figure 8B), where monomer and the H and J bands are represented (see below).

Figure 8B shows that the monomer absorption splits into two new bands in the dimer, one red shifted (λ_{max} 526 nm) of major intensity and the other blue shifted (λ_{max} 509 nm).

The monomer−dimer absorption spectrum can be interpreted through the exciton model.[51,52] According to this model the angle (α) and distance (R in Å) between the transition moment of the monomers in the dimer are defined by eqs 17 and 18, respectively

$$\alpha = 2 \arctan\sqrt{\frac{\nu_H f_J}{\nu_J f_H}} \quad (17)$$

$$R = \sqrt[3]{\frac{2.14 \times 10^{10} \cos \alpha f_M}{\Delta\nu\nu_M}} \quad (18)$$

where ν_x is the position of band X in cm^{-1} and f_X is the oscillator straight defined as $f_X = 1.3 \times 10^{-8}\Theta(n)\int_{-\infty}^{\infty}\varepsilon(\nu)d\nu$, $\Theta(n) = 9n/((n^2+2)^2)$ the factor of the environment, n the refraction index, and $\Delta\tilde{\nu}$ the difference of the positions of the split bands (J and H) in cm^{-1}.

The results obtained for K_D, α, and R for pigment **2** (Table 3) suggest that the interaction is a J-type aggregate as described in the literature.[51]

Conclusions

The reactions of four pyranoanthocyanin-flavan-3-ols and two pyranoanthocyanin−catechol pigments in hydroalcoholic aqueous solutions at different pH values were studied. These compounds were shown to not undergo hydration reactions but only acid−base reactions as recently described for vitisin B pigment. The acid−base equilibrium gives rise to three quinonoidal bases (neutral A, anionic A^-, and dianionic A^{2-}) between pH 3 and 12. The pK_a values obtained for all pigments were pK_{a1} between 4.20 and 5.35, pK_{a2} between 7.82 and 8.34, and pK_{a3} between 9.49 and 10.28. The first two pK_a values obtained agree with the ones available in the literature for natural and synthetic 7,4′-dihydroxyflavylium compounds. The third pK_a value (due to a proton transfer from (+)-catechin, (−)-epicatechin, or catechol unit) is also close to the respective values already reported. At wine pH (3.2−4.0) the pyranoanthocyanins studied are in their flavylium form AH^+ (red-orange color), and therefore, their contribution to the orange hues observed in aged wines could be important. Pyranomalvidin-3-*O*-coumaroylglucoside-(+)-catechin have shown the ability to form dimer and high-order aggregates at higher concentrations.

Acknowledgment. This research was supported by the research project grants (PTDC/QUI/67681/2006) and CONC-REEQ/275/2001 funding from FCT (Fundação para a Ciência e a Tecnologia) from Portugal. L.C. gratefully acknowledges the Ph.D. grant from FCT (SFRH/BD/30915/2006), and V.P. acknowledges the Postdoctoral Grant SFRH/BPD/18214/2004.

Supporting Information Available: Three figures that help to explain better the study of pyranoanthocyanin reactions in aqueous solutions and the aggregation phenomena of pigment **2**. This material is available free of charge via the Internet at http://pubs.acs.org.

References and Notes

(1) Rentzsch, W.; Schwarz, M.; Winterhalter, P. *Trends Food Sci. Technol.* **2007**, *18*, 526–534.
(2) Bakker, J.; Bridle, P.; Honda, T.; Kuwano, H.; Saito, N.; Terahara, N.; Timberlake, C. F. *Phytochemistry* **1997**, *44*, 1375–1382.
(3) Bakker, J.; Timberlake, C. F. *J. Agric. Food Chem.* **1997**, *45*, 35–43.
(4) Fulcrand, H.; Benabdeljalil, C.; Rigaud, J.; Cheynier, V.; Moutounet, M. *Phytochemistry* **1998**, *47*, 1401–1407.
(5) Cameira dos Santos, P. J.; Brillouet, J. M.; Cheynier, V.; Moutounet, M. *J. Sci. Food Agric.* **1996**, *70*, 204–208.

(6) Fulcrand, H.; Cameira dos Santos, P.; Sarni-Manchado, P.; Cheynier, V.; Favre-Bonvin, J. *J. Chem. Soc., Perkin Trans 1* **1996**, 735–739.
(7) He, J.; Santos-Buelga, C.; Silva, A. M. S.; Mateus, N.; De Freitas, V. *J. Agric. Food Chem.* **2006**, *54*, 9598–9603.
(8) Lu, Y. R.; Sun, Y.; Foo, L. Y. *Tetrahedron Lett.* **2000**, *41*, 5975–5978.
(9) Asenstorfer, R. E.; Hayasaka, Y.; Jones, G. P. *J. Agric. Food Chem.* **2001**, *49*, 5957–5963.
(10) Francia-Aricha, E. M.; Guerra, M. T.; Rivas-Gonzalo, J. C.; Santos-Buelga, C. *J. Agric. Food Chem.* **1997**, *45*, 2262–2265.
(11) Mateus, N.; Silva, A. M. S.; Santos-Buelga, C.; Rivas-Gonzalo, J. C.; De Freitas, V. *J. Agric. Food Chem.* **2002**, *50*, 2110–2116.
(12) Mateus, N.; Oliveira, J.; Haettich-Motta, M.; De Freitas, V. *J. Biomed. Biotechnol.* **2004**, 299–305.
(13) Mateus, N.; Silva, A. M. S.; Rivas-Gonzalo, J. C.; Santos-Buelga, C.; De Freitas, V. *J. Agric. Food Chem.* **2003**, *51*, 1919–1923.
(14) Oliveira, J.; De Freitas, V.; Silva, A. M. S.; Mateus, N. *J. Agric. Food Chem.* **2007**, *55*, 6349–6356.
(15) Oliveira, J.; Azevedo, J.; Silva, A. M. S.; Teixeira, N. r.; Cruz, L.; Mateus, N.; De Freitas, V. *J. Agric. Food Chem.* **2010**, *58*, 5154–5159.
(16) Cruz, L.; Teixeira, N.; Silva, A. M. S.; Mateus, N.; Borges, J.; De Freitas, V. *J. Agric. Food Chem.* **2008**, *56*, 10980–10987.
(17) Hakansson, A. E.; Pardon, K.; Hayasaka, Y.; de Sa, M.; Herderich, M. *Tetrahedron Lett.* **2003**, *44*, 4887–4891.
(18) Schwarz, M.; Jerz, G.; Winterhalter, P. *Vitis* **2003**, *42*, 105–106.
(19) SarniManchado, P.; Fulcrand, H.; Souquet, J. M.; Cheynier, V.; Moutounet, M. *J. Food Sci.* **1996**, *61*, 938–941.
(20) Mazza, G.; Minati, E. *Anthocyanins in fruits, vegetables and grains*; CRC Press: Boca Raton, FL, 1993.
(21) Brouillard, R.; Dubois, J. E. *J. Am. Chem. Soc.* **1977**, *99*, 1359–1364.
(22) Brouillard, R.; Delaporte, B. *J. Am. Chem. Soc.* **1977**, *99*, 8461–8468.
(23) Brouillard, R.; Delaporte, B.; Dubois, J. E. *J. Am. Chem. Soc.* **1978**, *100*, 6202–6205.
(24) McClelland, R. A.; Gedge, S. *J. Am. Chem. Soc.* **1980**, *102*, 5838–5848.
(25) Preston, N. W.; Timberlake, C. F. *J. Chromatogr.* **1981**, *214*, 222–228.
(26) Santos, H.; Turner, D. L.; Lima, J. C.; Figueiredo, P.; Pina, F. S.; Macanita, A. L. *Phytochemistry* **1993**, *33*, 1227–1232.
(27) Asenstorfer, R. E.; Iland, P. G.; Tate, M. E.; Jones, G. P. *Anal. Biochem.* **2003**, *318*, 291–299.
(28) Macanita, A. L.; Moreira, P. F.; Lima, J. C.; Quina, F. H.; Yihwa, C.; Vautier-Giongo, C. *J. Phys. Chem. A* **2002**, *106*, 1248–1255.
(29) Asenstorfer, R. E.; Jones, G. P. *Tetrahedron* **2007**, *63*, 4788–4792.
(30) Oliveira, J.; Mateus, N.; Silva, A. M. S.; De Freitas, V. *J. Phys. Chem. B* **2009**, *113*, 11352–11358.
(31) Pissarra, J.; Mateus, N.; Rivas-Gonzalo, J. C.; Santos-Buelga, C.; De Freitas, V. *J. Food Sci.* **2003**, *68*, 476–481.
(32) Cruz, L.; Borges, E.; Silva, A. M. S.; Mateus, N.; De Freitas, V. *Lett. Org. Chem.* **2008**, *5*, 530–536.
(33) Küster, W. F.; Thiel, A. *Tabelle per le analisi chimiche e chimico-fisiche*, 12th ed.; Hoepli: Milano, 1982.
(34) Mateus, N.; Carvalho, E.; Carvalho, A. R. F.; Melo, A.; Gonzalez-Paramas, A. M.; Santos-Buelga, C.; Silva, A. M. S.; De Freitas, V. *J. Agric. Food Chem.* **2003**, *51*, 277–282.
(35) Bax, A.; Subramanian, S. *J. Magn. Reson.* **1986**, *67*, 565–569.
(36) Bax, A.; Summers, M. F. *J. Am. Chem. Soc.* **1986**, *108*, 2093–2094.
(37) Mateus, N.; Silva, A. M. S.; Vercauteren, J.; De Freitas, V. *J. Agric. Food Chem.* **2001**, *49*, 4836–4840.
(38) Harborne, J. B.; Grayer, R. J. In *The flavonoids, advances in research since 1980*; Harborne, J. B., ed.; Chapman & Hall: London, 1988; pp 1−20.
(39) Beltrán, J. L.; Sanli, N.; Fonrodona, G.; Barrón, D.; Özkan, G.; Barbosa, J. *Anal. Chim. Acta* **2003**, *484*, 253–264.
(40) McClelland, R. A.; McGall, G. H. *J. Org. Chem.* **1982**, *47*, 3730–3736.
(41) Pina, F.; Melo, M. J.; Ballardini, R.; Flamigni, L.; Maestri, M. *New J. Chem.* **1997**, *21*, 969–976.
(42) Pina, F.; Melo, M. J.; Parola, A. J.; Maestri, M.; Balzani, V. *Chem.—Eur. J.* **1998**, *4*, 2001–2007.
(43) Pina, F.; Roque, A.; Melo, M. J.; Maestri, I.; Belladelli, L.; Balzani, V. *Chem.—Eur. J.* **1998**, *4*, 1184–1191.
(44) Slabbert, N. P. *Tetrahedron* **1977**, *33*, 821–824.
(45) Timberlake, C. F. *J. Chem. Soc.* **1957**, 4987–4993.
(46) Bergmann, K.; O'Konski, C. T. *J. Phys. Chem.* **1963**, *67*, 2169–2177.
(47) Monahan, A. R.; Blossey, D. F. *J. Phys. Chem.* **1970**, *74*, 4014–4021.
(48) Georges, J. *Spectrochim. Acta, A: M* **1995**, *51*, 985–994.
(49) Antonov, L.; Gergov, G.; Petrov, V.; Kubista, M.; Nygren, J. *Talanta* **1999**, *49*, 99–106.
(50) Antonov, L.; Petrov, V. *Anal. Bioanal. Chem.* **2002**, *374*, 1312–1317.
(51) Kasha, M.; Rawls, H. R.; Ashraf El-Bayoumi, M. *Pure Appl. Chem.* **1965**, *11*, 371–392.
(52) Mason, S. F. *J. Soc. Dyers Colour* **1968**, *84*, 604–612.

JP1045673